SARS-CoV-2 viral replication persists in the human lung for several weeks after onset of symptomatic severe COVID-19 and is associated with attenuated pulmonary immunity and variant-specific clinical sequalae

Tomasicchio M[1,2], Jaumdally S[1,2], Pooran A[1,2], Esmail A[1,2], Wilson L[1,2], Kotze A[1,2], Semple L[1,2], Meier S[1,2], Pillay K[5], Roberts R[5], Kriel R[5], Meldau R[1,2], Oelofse S[1,2], Mandviwala C[1,2], Burns J[1,2], Londt R[1,2], Davids M[1,2], van der Merwe[1,2] C, Roomaney A[1,2], Kühn L[1,2], Perumal T[1,2], Scott A.J[1,2], Hale M.J[6], Baillie V[7], Mahtab S[7], Williamson C[8], Joseph R[8], Sigal A[9], Joubert I[10], Piercy J[10], Thomson D[10], Fredericks DL[10], Miller MGA[10], Nunes M[7], Madhi S.A[7], Dheda K[1,2,3,4].

Affiliations:

[1] Centre for Lung Infection and Immunity, Division of Pulmonology, Department of Medicine, University of Cape Town and UCT Lung Institute, Cape Town, South Africa.

[2] South African MRC Centre for the Study of Antimicrobial Resistance, University of Cape Town, Cape Town, South Africa.

[3] Institute of Infectious Diseases and Molecular Medicine, University of Cape Town, Cape Town, South Africa.

[4] Faculty of Infectious and Tropical Diseases, Department of Immunology and Infection, London School of Hygiene & Tropical Medicine, London, UK.

[5] Division of Anatomical Pathology, Department of Pathology, University of Cape Town, Cape Town, South Africa

[6] Division of Anatomical Pathology, Faculty of Health Sciences, University of the Witwatersrand.

[7] South African Medical Research Council, Vaccines and Infectious Diseases Analytics Research Unit, Faculty of Health Sciences, University of the Witwatersrand, Johannesburg, South Africa; Department of Science and Technology/National Research Foundation South African Research Chair Initiative in

Vaccine Preventable Diseases, Faculty of Health Sciences, University of the Witwatersrand, Johannesburg, South Africa.

[8] Division of Medical Virology, Institute of Infectious Disease and Molecular Medicine, University of Cape Town, Cape Town, South Africa.

[9] Africa Health Research Institute, Durban, South Africa.

[10] Division of Critical Care, Department of Anaesthesia and Perioperative Medicine, University of Cape Town, South Africa

Correspondence: Keertan Dheda, Centre for Lung Infection and Immunity, Division of Pulmonology and UCT Lung Institute, Dept of Medicine, University of Cape Town, South Africa. E-mail: keertan.dheda@uct.ac.za

ABSTRACT

The immunopathogenesis of severe COVID-19 is incompletely understood. In contradistinction to the upper respiratory tract where replicating (culturable) SARS-CoV-2 is recoverable approximately ~ 4 to 8 days after symptom onset, there is paucity of data about the frequency or duration of replicating virus in the lower respiratory tract (the human lung). We undertook lung tissue sampling (needle biopsy), within ~2 hours of death, in 42 mechanically ventilated decedents during the Beta and Delta waves. Lung biopsy cores underwent viral culture, histopathological analysis, electron microscopy, transcriptomic profiling, immunohistochemistry and cell-based flow cytometry of deconstructed tissue. 38% (16/42) of patients had culturable virus in the lung (persisting for up to 4 weeks after symptom onset). This, hitherto, undescribed bio-phenotype of lung-specific persisting viral replication was associated with an enhanced pulmonary pro-inflammatory response and variant-specific increased rates of bacterial bronchopneumonia and accelerated death. These findings question existing paradigms and suggest that in a subset of patients, concurrent, rather than sequential active viral replication continues to drive a heightened pro-inflammatory response. Our findings have potential implications for the design of therapeutic interventional strategies and clinical management of severe COVID-19 disease.

Coronavirus disease- 19 (COVID-19) caused by the Severe Acute Respiratory Syndrome Coronavirus-2 (SARS-CoV-2) has been the foremost killer globally over the last 3 years. Case fatality risk (CFR) in hospitalised patients, and particularly in mechanically ventilated patients, during the Beta and Delta waves was particularly high (~50%-70%; [1]). Even with the Omicron-related variants, CFR remains significant in the elderly and immunocompromised persons, and in several countries including the UK, Italy, France, Brazil, and China where there is an unfolding epidemic of severe COVID-19 disease [2-10]. Better therapeutic interventions are needed. However, despite considerable research, the pathogenesis of severe COVID-19, relative to viral kinetics, remains incompletely understood.

SARS-CoV-2 detection (ascertained through PCR positivity or antigen detection) can persist for several weeks from symptom onset [11]. Indeed, postmortem studies have shown persistence of SARS-CoV-2 in tissues detected by PCR and immunohistochemistry for up to several weeks after symptom onset [12,13]. Detection of SARS-CoV-2 in these studies may not represent replication competent virus (detectable only by viral culture) but residual genomic or antigenic material in the tissues. However, shedding of replicating virus confirmed through serial viral culture (i.e. *in vitro* replication in human cell lines) from the upper respiratory tract (URT) has been shown to persist for only ~2 to 8 days after symptom onset [11,14-23]. These findings were confirmed in human lung challenge studies where virus was cultured from the upper respiratory tract until a median of 4 days (and a maximum of 10 days) from symptom onset [24]. However, hardly anything is known about the compartment-specific duration of actively replicating virus in the lower respiratory tract (LRT), particularly in severely ill hospitalised patients undergoing mechanical ventilation. We hypothesised that there is compartment-specific uncoupling of viral replication in severe COVID-19 i.e. replicating virus can persist in the LRT beyond 10 days from symptoms onset, independent of its persistence in the URT, and this persistence may be associated with an altered pulmonary immunity.

The widely accepted view in severe COVID-19 is that resolution of the initial viraemic phase in the first week after symptom onset is followed by an effector or hyperinflammatory phase in the second and third week of illness, characterised by diffuse alveolar damage, thrombo-inflammation, and endotheliopathy [25]. Indeed, the Infectious Disease Society of America (IDSA) recommends the use of remdesivir for only 5 days in patients with severe illness [26]. However, our results based on postmortem lung biopsies obtained using minimally invasive tissue sampling (MITS; within ~2 hours after death) methods indicated that, in contradistinction to the URT where replication often ceases in the human lung, virus is culturable in ~40% of mechanically ventilated patients until death (median of 15 days and up to 4 weeks after symptom onset; see Figure 1 for the study overview). Nasopharyngeal SARS-CoV-2 viral load (based on Ct value) at admission or at death, was not associated with likelihood of lung culture positivity. SARS-CoV-2 culture in the lung of decedents was associated with attenuated pulmonary T-cell immunity and an exaggerated pro-inflammatory phenotype.

We first ascertained the frequency and duration of replicating virus in lung tissue (which to our knowledge has not been previously undertaken). Culturable virus was present in 38.1% (16/42; Figure 2A) of mechanically ventilated ICU decedents, at a median of 15 days (and up ~4 weeks) from symptom onset to sampling/death (Figure 3A). By contrast, in a prospectively recruited control group of ambulatory patients 5.5% (1/18) and 0% (0/18) had culturable virus, using nasopharyngeal swab samples, at day 12 (p=0.01) and 19 (p=0.002) after symptom onset, respectively (Figure 2B). Additionally, SARS-CoV-2 could be detected by PCR in multiple organs in lung culture-positive decedents in the Delta cohort (biopsies other than the lung was not performed in the Beta cohort) suggesting widespread multi-organ viral dissemination (Figure 2C). SARS-CoV-2 was also detected in the adipose tissue of culture positive decedents (hitherto undescribed) and associated with fat necrosis (Table S2). Clinical characteristics such as age and comorbidities were similar in the lung culture-positive versus culture-negative groups (Table S1) and we found no association between viral genetic variant and the phenotype of replicating viral persistence (although this might have been a factor of the limited sample size; Table S4).

Collectively, these findings challenge the traditional paradigm of an initial viral replicative phase roughly in the first week of severe illness sequentially followed by an effector or inflammatory phase [25]. Our data suggest that in ~40% of ventilated patients, viral replication persisted until death (i.e. 3rd and 4th week of illness and at a median of 15 days after symptom onset). This challenges the current practice of using antivirals like remdesivir for only ~5 days and suggests that a longer duration of treatment may be required in critically ill patients. Furthermore, remdesivir is not recommended for use by IDSA in mechanically ventilated patients (conditional recommendation) as it felt that such patients (often in the third week of their illness) are no longer in the viral replicative phase, and published controlled trial data showed no mortality benefit of remdesivir in such patients [26,27]. However, these analyses did not adjust for disease severity or the time from symptom onset to death in mechanically ventilated patients [28]. Our data suggest that a significant number of patients would likely benefit from antivirals during mechanical ventilation, and these findings challenge current recommendations. Indeed, several observational studies have found a survival benefit using remdesivir in mechanically ventilated patients, but this requires further clarification in appropriate trials [28-30]. Our findings also raise the possibility that steroids (discussed further below), although beneficial, may be prolonging viral replication in some patients (generally used for 7 to 10 days in severe disease) though this requires further clarification in *in vitro* studies.

Next, we interrogated whether nasopharyngeal PCR characteristics (Ct value), either at admission or close to death, could identify the phenotype of lung replicating viral persistence. However, nasopharyngeal Ct neither at admission, nor at the time of death was associated with lung culture positivity (Figure 3G). This suggests that the kinetics of viral replication is different in the upper and the lower respiratory tract.

Next, we evaluated variant-specific relationships to clinical outcomes. Mechanically ventilated patients that were SARS-CoV-2 lung culture-positive in the Delta, but not in the Beta cohort, had accelerated

death (i.e. shorter duration from symptom onset to death; Figure 3C versus 3B; p=0.004), higher rates of concurrent bacterial bronchopneumonia (Figure 3F versus 3E; p=0.037), and a higher proportion of lung-specific secondary bacterial infection (Figure S4C versus S4B; p=0.022) compared to culture-negative persons. Clinical and demographic characteristics could not explain these observations, and this was despite the lower population-level vaccination and pre-existing COVID-19 exposure rates in the Beta cohort. It is possible that Delta was associated with more profound lung-specific immune attenuation (however, sample sizes were too small to reliably make this comparison; discussed below). Steroid usage differentially driving viral replication is unlikely to explain the findings in the culture-positive group as steroid usage was significantly higher in the culture-negative group (Table S1; p=0.047).

Next, we sought to ascertain whether the phenotype of replicating viral persistence was associated with attenuated or modulated lung immunity in the Delta decedents (transcriptomic and flow cytometric studies were only carried out in Cape Town, i.e the Delta decedents, due to location-specific availability of assays and limited Beta group biopsy cores that had been used for unrelated studies). Immunohistochemical staining indicated that there was significantly less infiltration of CD4+ T-cells/macrophages and CD8+ T-cells in the alveoli and interstitium of the SARS-CoV-2 culture-positive compared with the culture-negative individuals in the Delta decedents (Figure 4A and B; immunohistochemical staining was not performed in the Beta cohort due to limited sample availability as outlined above). This was in keeping with an attenuated CD4+ and CD8+ Th1 response seen in cells obtained from deconstructed lung tissue of the Delta group descendants using flow cytometry (Figure S6).

The lung-specific transcriptional analysis (to our knowledge, hitherto, not undertaken in patients with severe COVID-19) at individual gene level identified 630 up- and 885 downregulated genes when comparing the culture positive versus negative groups. The 630 significantly upregulated genes

highlighted pathways that were associated with a proinflammatory response related to cytokine signalling, neutrophil and monocyte chemotaxis/ recruitment, and viral entry/ defence, all implicated in COVID-19-related hypercytokinaemia [31] (Figure 5, S7 and S8, Table S5 and S6A). The 885 downregulated pathways were mostly associated with body homeostasis (Figure 5A and B). The same comparison after adjustment for multiple testing, identified a total of 11 up- and 5 down-regulated genes in the culture-positive compared to culture -negative individuals at (FDR<0.05; specific genes discussed further in the online supplement). There was also in tandem upregulation of Th1 and Th17 signalling pathways (Figure S6B) but to a substantially lesser extent than that of innate cellular and signalling pathways (IL-1, IL-6 and neutrophil-related). These features may be consistent with an aberrant immune response (including lack of activation of regulatory and immune-suppressive pathways). We did not see a pattern consistent with T-cell exhaustion (upregulation of markers such as PD-1, CTLA-4, LAG etc., Table S6C) known to be associated with severe COVID-19.

Next, we evaluated whether any of the differentially expressed genes could act as biomarkers discriminating between lung culture-positive and negative-individuals. Logistic regression predictive modelling revealed that *GREM1* and *FGFBP1* were associated with a sensitivity and specificity above 90% (further details in the online supplement). Although these are lung-specific biomarkers, this preliminary analysis in a limited number of samples suggest that in the future, RT-PCR of tracheal aspirates, or blood (if they are found to be concordant with lung findings), could potentially serve as biomarkers to identify and direct appropriate treatment to culture positive persons. This will need to be further investigated in future studies.

Collectively, these data suggest that in a significant number of patients the hyperinflammatory and viraemic phase occur concurrently in the 3rd and 4th week of illness, in contradistinction to the widely held view that these are sequential phases. Antiviral and selective proinflammatory responses were overrepresented in the SARS-CoV-2 culture-positive compared with the culture-negative decedents,

and we did not detect attenuated type 1 interferon responses at the site of disease compared with other reports, though these looked at peripheral blood rather than lung responses [32-34].

The typical histological features of severe COVID-19 (e.g. diffuse alveolar damage and microvascular thrombosis) were similar in the SARS-CoV-2 culture-positive compared with the culture-negative phenotype suggesting that these events occurred in the early rather than the persistent viraemic phase (Figure 4C and D). However, pneumocyte proliferation was higher in the culture-negative cohort versus the culture-positive cohort (Figure 4C; p=0.024). Interestingly, we also observed that some features of leucocyte hyperactivation (i.e., hemophagocytic syndrome) were more common in the SARS-CoV-2 culture-negative versus the culture-positive group, potentially in keeping with an aberrant immune response characterised by a lack of immune regulation, as outlined above (Figure 4C; p=0.008).

There are several limitations to our findings. Firstly, our findings are relevant to severe COVID-19 ARDS/pneumonia requiring mechanical ventilation and may not be applicable to milder forms of disease seen in hospitalised patients. Second, we only studied patients with the Beta and Delta variants. However, Omicron has also been associated with severe disease in several settings including the surge of severe COVID-19 unfolding in China. Third, we did not study a control group comprising severe ARDS due to other causes. However, our express aim was to investigate the presence and duration of viral replication in the LRT in severe COVID-19. Fourth, the sample size limited our ability to make conclusions about several aspects. However, the resource intensive and demanding nature of the study limited our ability to recruit higher numbers of participants. Finally, the transcriptional signature and flow cytometric findings may have been affected by post-death sampling in the Delta decedents. However, several detailed studies have shown [35] that most protein and RNA species are preserved and stable for several hours after death. Given that biopsies for the transcriptional studies were generally taken within 2 hours after death, we feel they are broadly representative of the picture at the time of death.

In summary, our data suggest that there is considerable heterogeneity in the duration of viral replication in the upper versus the lower respiratory tract beyond the 2nd week of illness, and that in a significant proportion of seriously ill patients, persisting viral replication occurs concurrently and may drive an exaggerated proinflammatory response (higher than in culture negative persons), rather than sequentially as it is widely believed. These findings have implications for the use of antiviral therapy in seriously ill patients with COVID-19 and suggest that better biomarkers are needed to identify patient phenotypes and subsets that might benefit from concurrent anti-inflammatory and antiviral therapy.

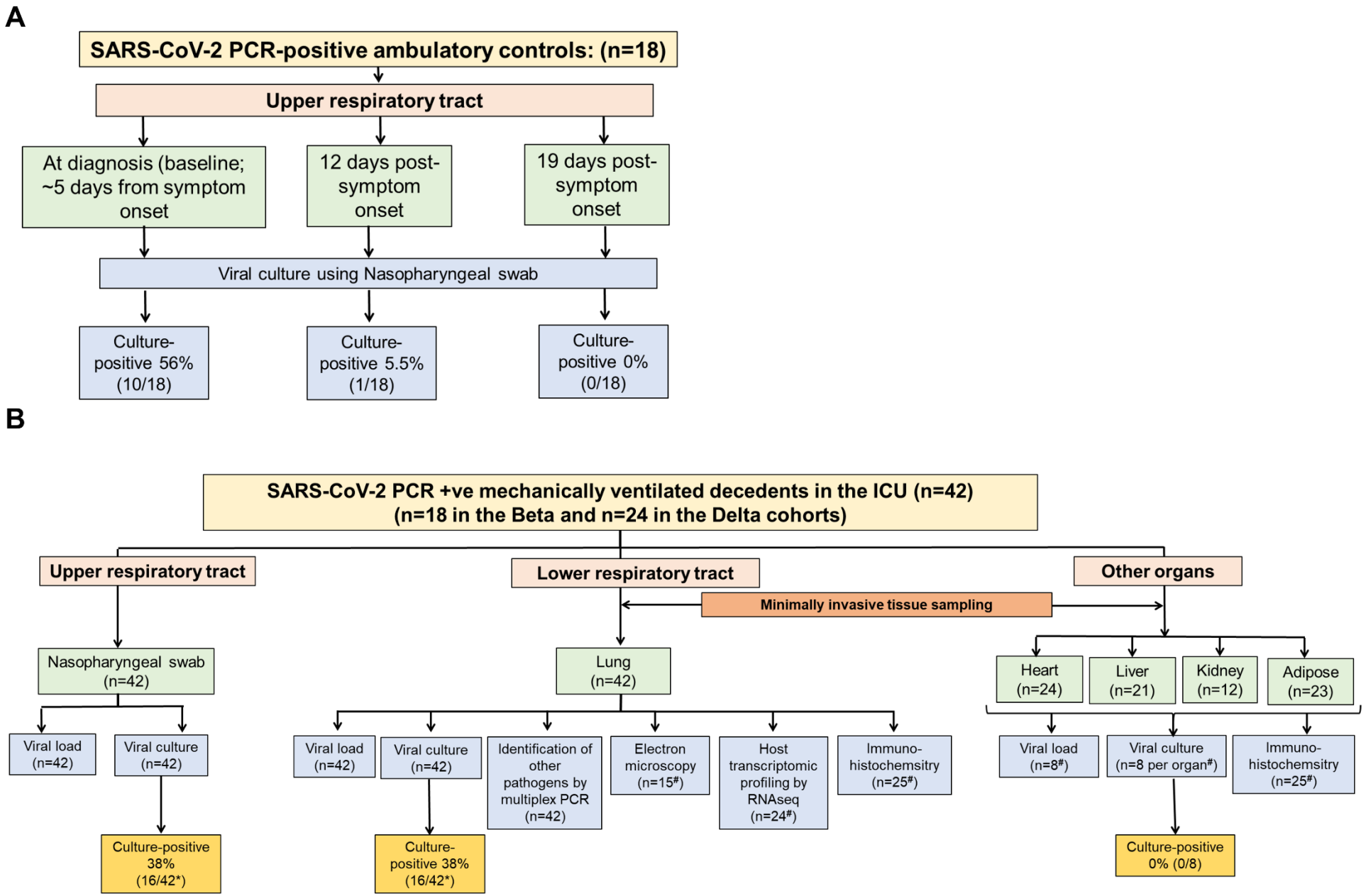

*The 16 decedents that were nasopharyngeal culture-positive were not the same patients that were lung culture-positive. #Immunohistochemistry, RNAseq, electron microscopy and viral culture of other organs was only performed on the Delta cohort.

Figure 1. Study overview including SARS-CoV-2 PCR-positive ambulatory controls (A) and mechanically ventilated decedents (B) recruited during the Beta and Delta waves. Nasopharyngeal (NP) swabs from ambulatory COVID-19 controls were obtained approximately 5 days after symptom onset (diagnosis), and then at 12- and 19-days post symptom onset. Minimally invasive tissue samples (MITS) and NP swabs were retrieved from decedents within 2 hours post death.

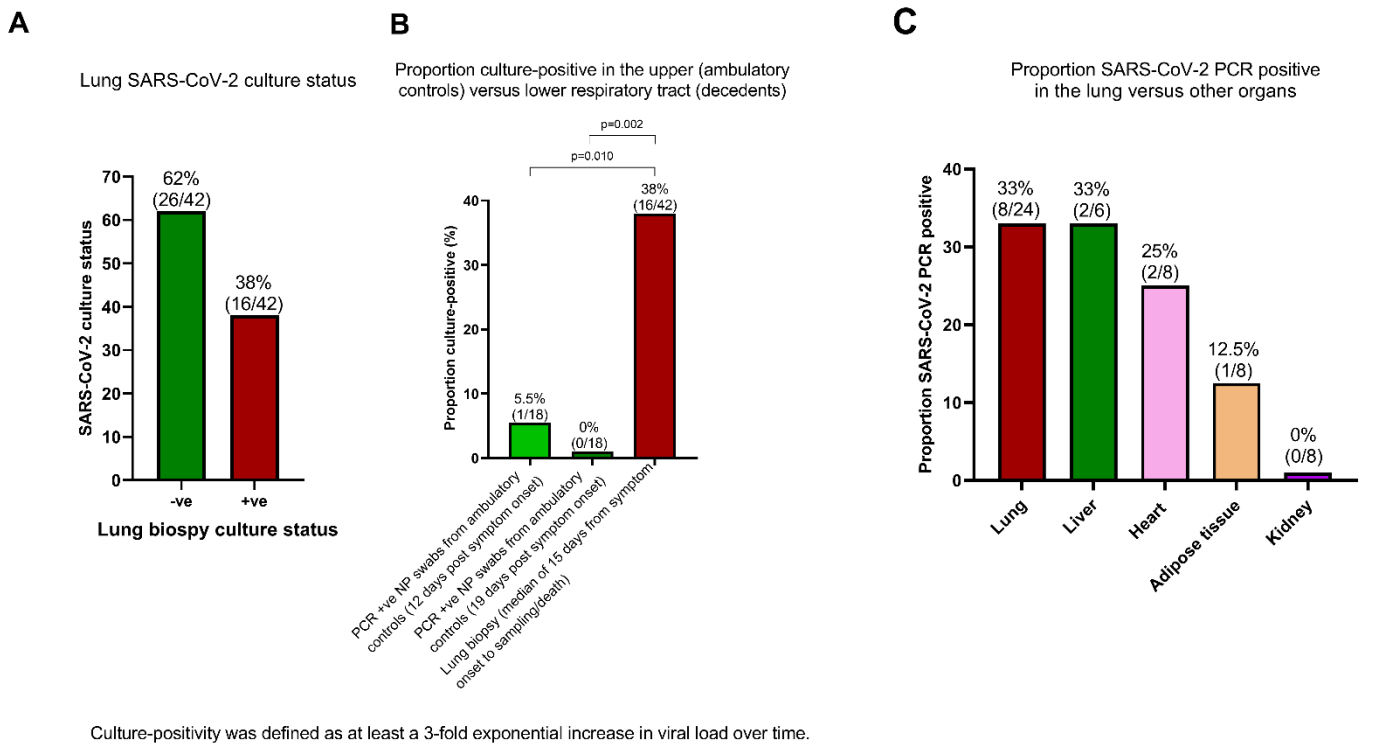

Figure 2. Active replicating virus was recovered from the lungs of over one third of decedents (16/42). (A) Proportion of lung biopsy samples that were culture positive. **(B)** Proportion of serial nasopharyngeal swabs from PCR-positive ambulatory controls compared to lung biopsy samples from culture-positive decedents. **(C)** PCR positivity of organs of lung culture-positive decedents from the Delta cohort. NP= nasopharyngeal.

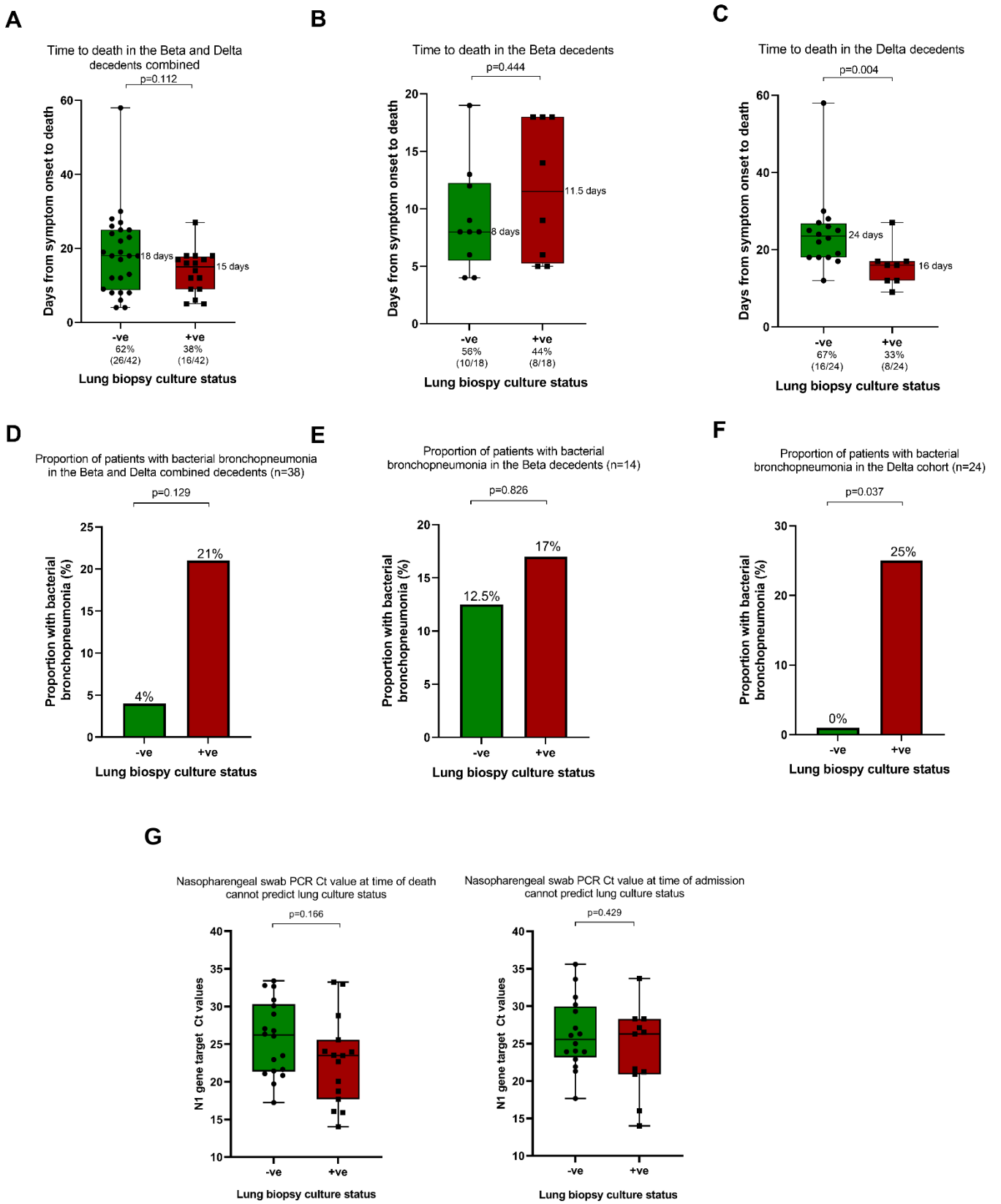

Figure 3. The phenotype of replicating viral persistence, compared to the culture-negative participants, was associated with accelerated death and a higher frequency of bacterial bronchopneumonia in the Delta but not the Beta group. (**A**) The days from symptom onset to death for the culture-negative (-ve; green) and culture-positive (+ve; red) groups for both groups combined, and for the Beta (**B**) and Delta (**C**) groups alone. Proportion of samples/ participants with microbiologically and histologically confirmed bacterial bronchopneumonia in culture-negative and culture positive decedents overall i.e. the combined groups (Beta and Delta) (**D**), Beta group only (**E**), and Delta group only (**F**). **(G)** PCR cycle threshold (Ct) value at the time of death or at admission could not discriminate or predict lung culture status.

A

A greater proportion of CD3+ T-cells, CD4+ T-cells/macrophages and CD8+ T-cells infiltrate into the alveoli and interstitial space in culture-negative compared to culture-positive individuals in the Delta decedents

	Lung culture status		
Frequency of infiltration into the alveoli	**-ve (n=11[#])**	**+ve (n=7*)**	**p value**
CD3+			
Medium	55% (6/11)	0% (0/7)	**0.017**
High	0% (0/11)	0% (0/7)	N/A
CD4+			
Medium	45.5% (5/11)	57% (4/7)	0.644
High	45.5% (5/11)	0% (0/7)	**0.036**
CD8+			
Medium	54.5% (6/11)	0% (0/7)	**0.017**
High	0% (0/11)	0% (0/6)	N/A
CD68+			
Medium	36.4% (4/11)	14.3% (1/7)	0.322
High	36.4% (4/11)	43% (3/7)	0.786

CD68 (macrophage marker)

B

Representative images showing CD3+ T-cells, CD4+ T-cells/macrophages and CD8+ T-cells infiltration into the alveoli and interstitial space of the lung in culture-negative compared to culture-positive individuals in the Delta decedents

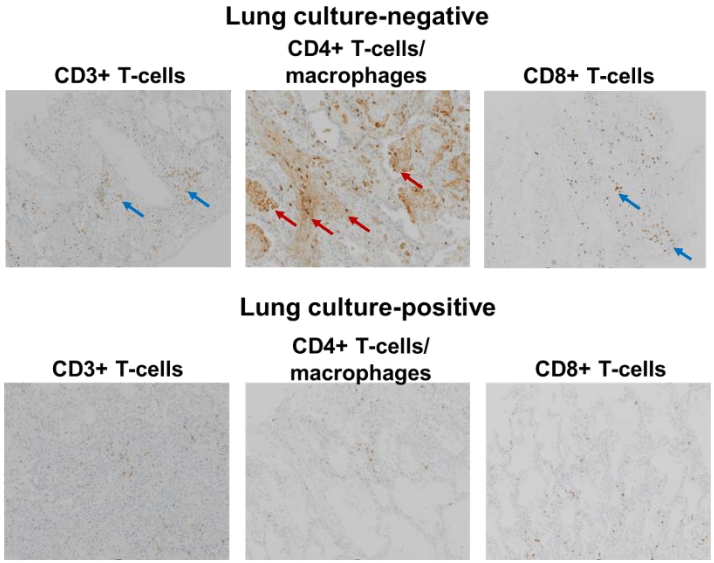

C

A greater proportion of type II pneumonocytes proliferation and haemophagocytosis was observed in the alveoli of the culture-negative compared to culture-positive individuals in the Delta group

	Lung culture status		
Lung histology	**-ve (n=20♠)**	**+ve (n=13♣)**	**p-value**
Alveolar hyaline membranes	16/20 (80%)	8/13 (61.5%)	0.245
Microvascular thrombosis	6/20 (30%)	5/13 (38.5%)	0.614
Organising hyaline membranes	9/12 (75%)	6/7 (86%)	0.581
Type II pneumocytes proliferation	20/20 (100%)	10/13 (77%)	**0.024**
Organising pneumonia	6/20 (30%)	4/13 (31%)	0.963
Lung haemophagocytosis	14/20 (70%)	3/13 (23%)	**0.008**

D

Both culture-positive and culture-negative decedents present with histopathological findings typically associated with SARS-CoV-2 pneumonia

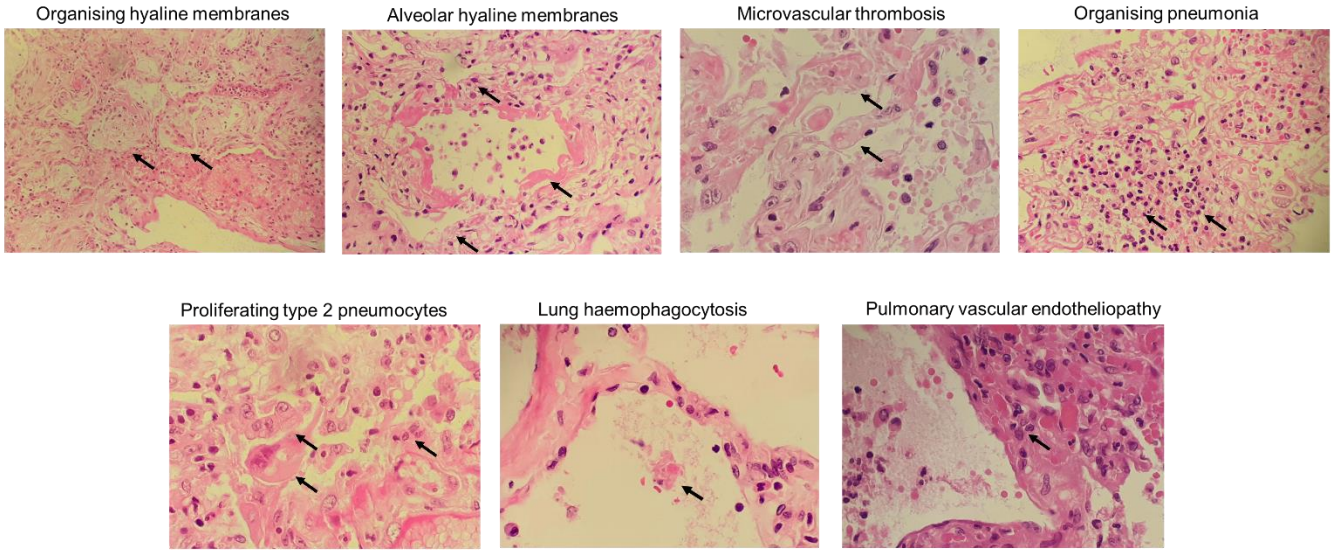

[#]IHC was not performed on 5 culture-negative samples. [*]IHC was not performed on 1 culture-positive sample. [♠♣]Histology was not performed on all the biopsy samples. N/A = not applicable .

Figure 4. A higher proportion of T-cells, macrophages and pneumonocytes infiltrate into the lung of the culture-negative versus culture-positive decedents in the Delta group. (A) More T-cells infiltrate into the alveoli and interstitial space of the lung culture-negative versus culture-positive group in the Delta decedents as assessed by immunohistochemistry. **(B)** Representative images (immunohistochemistry) showing better T-cell infiltration into the alveoli (red arrow) and interstitial space (blue arrow) in the lung culture-negative versus the culture-positives in the Delta cohort. Histopathology findings **(C)** and representative images **(D)** associated with diffuse alveolar damage and microvascular thrombosis in the Delta decedents. The black arrows indicate key histopathological features.

The culture-positive, group compared to the culture-negative group, was associated with the enrichment of inflammatory, innate immune and enhanced SARS-CoV-2 entry pathways

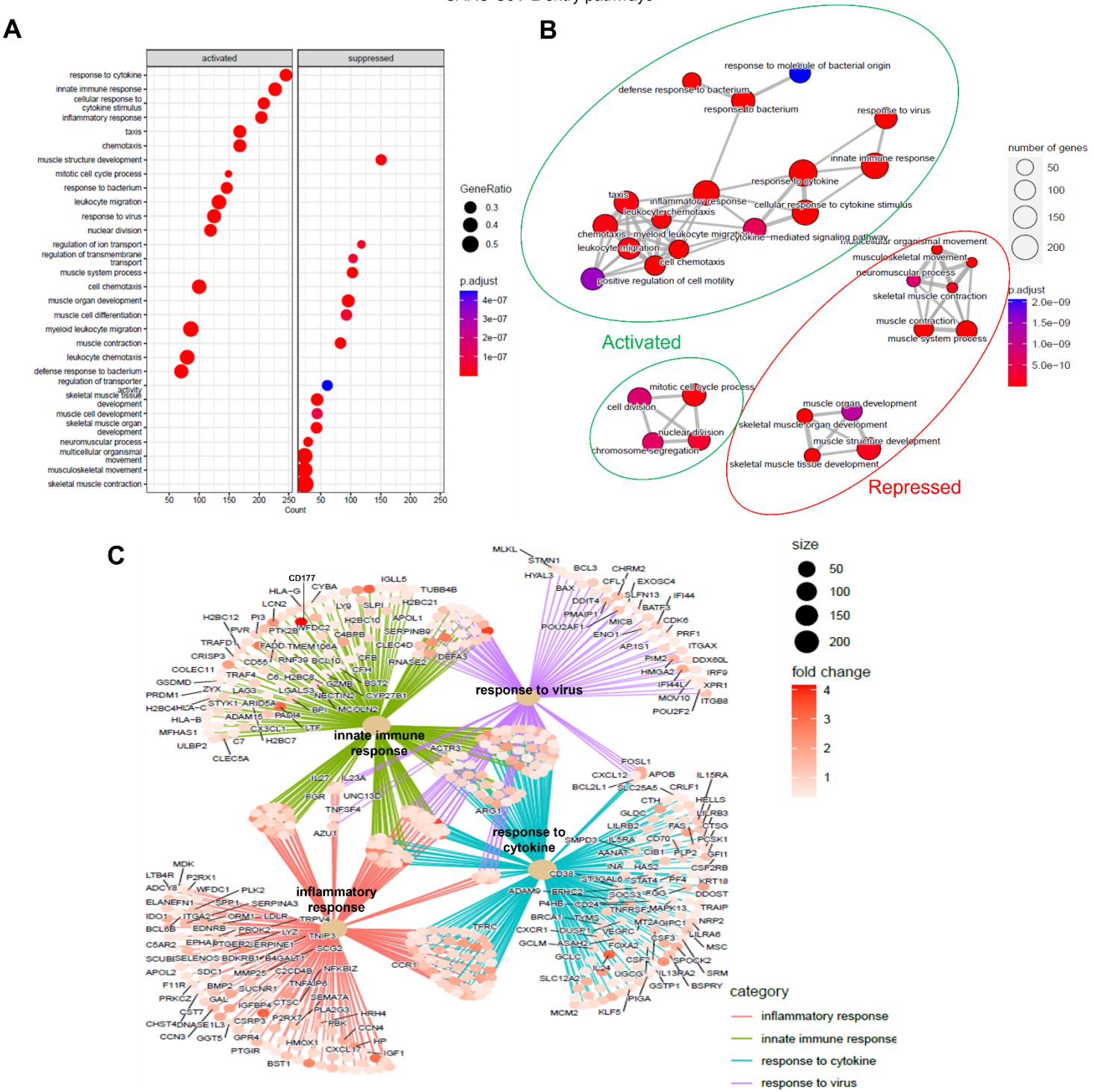

Figure 5. The transcriptomic analysis revealed that the culture-positive group, in comparison to the culture negative group, had enrichment of activated pathways associated with inflammation, innate immunity, responses to cytokines, and responses to virus/ bacterial stimuli in the Delta descendants. Dot plot illustrating the significantly activated and suppressed pathways along with the gene count and ratio for each pathway (**A**), enrichment map illustrating the significantly activated and suppressed pathways along with the gene count and ratio for each pathway (**B**) and cnetplot similarly illustrating the overlap of genes and their fold changes for selected activated pathways (**C**).

ONLINE MATERIALS AND METHODS.

Patients.

The decedents (n=42) were recruited from Chris Hani Baragwanath Academic Hospital, Johannesburg, South Africa (n=18; Beta group) and Groote Schuur Hospital, Cape Town, South Africa (n=24; Delta group). Ethical approval was obtained from the Human Research Ethics Committee (HREC) of the University of Cape Town (HREC approval number 866/2020) and University of Witwatersrand (HREC approval number M200313). Biosafety approvals were obtained from the Faculty Biosafety Committee of the University of Cape Town (IBC008-2021).

Viral culture.

To establish the *in vitro* viral culture model, a SARS-CoV-2 viral stock was used to infect the human lung carcinoma cell line, H1299, in a BSL3 laboratory and infection was confirmed by light microscopy (as assessed by cytopathic effects of the virus on the cell line) and confocal microscopy (Figure S1A and B). Serial dilutions of the viral stock were used to establish the limit of detection of the PCR assay at 1×10^1 copies/ml (Figure S1C). Viral culture was performed on the nasopharyngeal swab and lung biopsy samples as indicated in the study overview (Figure 1). The cell line was maintained in Roswell Parks Memorial medium (RPMI) containing 10% bovine serum, 100 IU penicillin/streptomycin, 2 mM L-glutamine, 25 mM HEPES, 1x non-essential amino acids and 0.1 mg/mL sodium pyruvate (ThermoFisher, South Africa; Figure S1). The NP swabs in universal transport medium (UTM) were initially filtered through a 0.22µm filter prior to inoculation. The lung biopsy samples were placed in the well containing the cellular monolayer. The inoculated cultures were grown in a humidified 37°C incubator with 5% CO_2 and cytopathic effect (CPE) and viral replication were monitored on days 1, 3, 6 and 9 by PCR. Viral culture positivity was defined as at least a 3-fold increase in viral load over time.

Multiplex PCR to detect secondary bacterial infections.

The lung biopsy cores stored in UTM were briefly homogenised and 200µl of the supernatant was applied to the BioFire® FilmArray® Pneumonia panel (Bioméieux, South Africa). The panel was run using protocol BAL v3.3 according to the manufacturer's instructions, thus generating RT-PCR readouts for 33 bacterial and viral pathogens. Bronchopneumonia was defined as histological evidence of a neutrophilic alveolar infiltration together with the detection of bacterial genomic material in the biopsy cores.

Immunohistochemistry.

Immunohistochemical staining was performed using the Roche Ventana Automated platform (Ventana XT autostainer). Sections between 3-4um thick were placed on adhesive slides and fixed at 37°C overnight. Heat induced epitope retrieval (HIER) time was set to 60 minutes to prevent tissue wash off and possible background staining. The antibodies (CD3 [2GV6], CD4 [SP35], CD8 [SP57] and CD68 [KP-1]; Roche USA) were incubated with the tissue sections for 30 minutes. After antibody and counter staining, slides were visualised using an Olympus BX41 microscope at 40x magnification.

Haematoxylin and eosin staining.

The specimens were received in labelled plastic specimen containers containing 10% buffered formalin. The specimen was carefully removed from the container using a pour-over technique and/or small forceps with minimal pressure. The specimen was wrapped in a small fragment of teabag paper (JoyPak Contract Packaging Company, Cape Town) and placed in the appropriate labelled tissue cassette. The lid of the cassette was tightly closed to ensure that the specimen was secure. The tissue block was placed in a tray containing 10% buffered formalin and transferred to the automated tissue processor (Tissue Tek VIP 5E-F2-VIP1). The tissue blocks underwent overnight processing (start time 16:00, end time 06:00) through a multistep process of being exposed to formalin, 96% alcohol, 100% alcohol, xylol, wax and water. This process occurred at temperatures ranging from 37–60°C. The end point of tissue processing was the formation of a formalin-fixed paraffin embedded tissue block containing the specimen. The chilled wax block was placed on a microtome chuck and the tissue blocks were sectioned to 3-4um thickness. The block was trimmed, and folds removed by placing the section into a water bath. The section was orientated in the water bath and placed onto a coated slide. The slides are stained with haematoxylin and eosin (H&E) and viewed using an Olympus BX43 microscope at 2x-40x magnification.

Transmission electron microscopy.

Tissue specimens preserved in glutaraldehyde were trimmed/cut as thinly as possible under a stereomicroscope and placed into a specimen basket. The basket was then placed into a tissue processor and processed from glutaraldehyde through osmium tetroxide, uranyl acetate, increasing concentrations of alcohol and finally to resin. The tissue samples were then placed into labelled embedding capsules and filled with resin. The resin blocks were put into an incubator to set overnight.

Once the resin blocks had set, using the ultra-microtome, thick (0.5µm) sections were cut into a water bath and placed onto coated glass slides which were stained with toluidine blue. A mesa block with the relevant area of tissue was cut on the resin block which the thin (0.1 µm) sections were then cut from. The thin sections were placed onto a copper grid and once dried were stained with saturated uranyl acetate in sterile water and counterstained with lead citrate. Once the copper grids had dried, they were placed into the Carl Zeiss EM109 electron microscope for screening.

SARS-CoV-2 whole genome sequencing.

Total SARS-CoV-2 RNA was extracted from lung biopsy samples using the ChemagicTM 360 automated system (PerkinElmer, Inc, Waltham, MA) and carried out according to the chemagic Viral300 360 H96 drying prefilling VD200309.che protocol. Whole genome amplification and library preparation were performed using the Illumina COVIDSeq Test kit and protocol 1000000128490 v02 (Illumina, Inc., San Diego, CA), and executed on the Hamilton Next Generation StarLet (Hamilton Company). Whole genome amplification was achieved via multiplex polymerase chain reaction performed with the ARTIC V4.1 primers designed to generate 400-bp amplicons with an overlap of 70 bp that spans the 30 kb genome of SARS-CoV-2. Indexed paired-end libraries were normalized to 4 nM concentration, pooled, and denatured with 0.2 N sodium acetate. A 4pM pooled library was spiked with 1% PhiX Control v.3 adaptor-ligated library (Illumina, Inc., San Diego, CA) and sequenced using the MiSeq® Reagent Kit v2 (500 cycle) and sequenced on the MiSeq instrument (Illumina, Inc., San Diego, CA). The quality of sequencing reads was assessed using different tools including FastQC, Fastp, Fastv, Fastq_screen, and Fastx_toolkit. The resulting reads were analyzed on Exatype (https://exatype.com/) for referenced-based genome assembly and to identify minor and major variants. The assembled consensus sequences were analyzed using Nextclade Web (https://clades.nextstrain.org) for further quality control and clade assignment.

RNAseq.

RNAseq was performed on lung post-mortem biopsy samples from 24 individuals which included 8 that were COVID culture-positive and 16 that were culture-negative.

Total RNA was extracted from lung biopsy samples using the RNeasy mini plus kit (Qiagen). Ribosomal depletion was performed, and libraries were prepared using the MGIEasy RNA Library Prep Set (Cat. No.: 1000006383, 1000006384, MGI, Shenzhen, China) as per manufacturer's instructions. Sequencing was performed at the South African Medical Research Council Genomics Centre using DNA nanoball-based technology on the DNBSEQ-G400 (BGI, Shenzhen China) instrument generating 100 bp unstranded paired-end reads. The FastQC program (version 0.11.9) [36], was used to assess read quality. The Spliced Transcripts Alignment to a Reference (STAR) software (version STAR_2.7.7a) [37] was used to map reads to the Ensembl [38] human genome primary assembly (version GRCh38.99) with the quantMode and GeneCounts option selected to generate raw genewise read counts for each sample. A number of samples failed to pass QC due to a low number of mapped reads (< 2 million). A total of six culture positive and five culture negative samples were used in subsequent analysis.

The differential expression (DE) analysis was performed with the edgeR (version 3.38.4) [39] Bioconductor [40] package. Briefly, raw counts were filtered to remove genes with low expression, normalized, and negative binomial generalized linear models were fitted. The likelihood ratio test was used to identify DE genes when comparing culture-positive to culture-negative samples.

Confocal microscopy.

The H1299 cells were plated and allowed to adhere to coverslips slides overnight at 37°C. The next day the cells were stained with or without anti-SARS-CoV-2 S1 spike protein (ThermoFisher, USA) and the slides were mounted in Mowiol (Calbiochem, USA) containing n-propyl gallate (Sigma-Aldrich, Germany) as anti-fading agent. Confocal microscopy was performed with a Zeiss Axiovert 200M LSM 510 Meta NLO Confocal Microscope using the 40X water immersion objective and the 63X oil-immersion objective.

Lung tissue digestion and flow cytometry.

The lung biopsy sample was cut into 1 mm by 1 mm pieces using a scalpel in a BSL2 cabinet. The cut pieces were placed in 1 ml hanks balanced salts (HBSS; Lonza, Germany) containing 5 µg/ml Collagenase II (Ambion, USA) and the tissue was digested by incubation at 37°C with rotation for 45 min. After the incubation time the undigested tissue was discarded using a 0.7 µM cell strainer (Becton Dickinson, USA). The cell strainer was washed with 10 ml of HBSS and the cells were pelleted at 500 × g for 5 min.

Prior to antibody staining the cells were stained with the fixable viability dye, Zombie (Biolegend, USA) in PBS. The cells were stained with antibodies against CD3, CD4, CD8, IFN-γ, TNF-α, IL-2 and IL1-β (Biolegend, USA), Approximately $1x10^5$ cells were acquired using a LSRII Flow Cytometer (Becton Dickinson, USA) and the data analysed using FloJo software (version 10.1; Treestar, USA). Dead cells were excluded from the scatter plots prior to analysis, and negative gates were set using fluorescence minus one (FMO) controls. Only the single cellular population was analysed.

Statistical analysis.

The chi-squared ($\chi 2$) test was employed for categorical variables and for continuous variables, Mann-Whitney test was used for non-parametrically distributed data (Stata version 17 or GraphPad, Version 9.4.1). A p-value of < 0.05 was considered significant for all statistical analyses. The DE results were sorted/ranked by fold change and a gene set enrichment analysis (GSEA) for Gene Ontology (Biological Process) and KEGG pathways was performed using the gseGO and gseKEGG functions respectively, from the clusterProfiler (ver: .4.4.4; [41]) package in R. Pathways with an FDR <0.05 were considered significant.

ACKNOWLEDGMENTS.

The authors would like to thank Arnold-Day C, Crowther M, Fernandes N, and Mitchell L from the Division of Critical Care, Department of Anaesthesia and Perioperative Medicine, University of Cape Town, South Africa for identifying and referring potential patients into the study. **Funding:** The study was funded by the Bill & Melinda Gates Foundation (grant number INV-017282) and the South African Medical Research Council (grant number SHIP NCD 96756) with partial support from the Department of Science and Technology and National Research Foundation: South African Research Chair Initiative in Vaccine Preventable Diseases. The KD lab acknowledges funding from the SA MRC (RFA-EMU-02-2017), EDCTP (TMA-2015SF-1043, TMA-1051-TESAIII, TMA-CDF2015), UK Medical Research Council (MR/S03563X/1), NIH (CRDF-OISE-16-62105) and the Wellcome Trust (MR/S027777/1). **Author contributions:** K.D, MT, S.J, A.P, A.E, M.D, M.N and S.M conceived and designed experiments. K.D, A.E, S.O, L.K, T.P, A.S, I.J, J.P, D.T, D.F, A-D C, M.M, M.C, N.F, L.M, M.N and S.M arranged medical ethical approval, recruitment of study participants and collection of study material. MT, SJ. A.P, L.W, A.K, S.M, K.P, R.R, R.K, R.M, C.M, J.B, R.L, M.D, C vdM, A.R, M.H, V.B, S. M, C.W, and R.J performed the experiments. M.T, S.J, A.P and M.D set up experimental assays. A.S provided the cell line. K.D, M.T, S.J, A.P, L.W, A.K, L.S, S.M, K.P, R.R, R.L, M.H, V.B, S.M, R.J, and N.M analysed and interpreted data. K.D, M.T, L.S, and S.M wrote the manuscript with input from all listed authors **Competing interests:** The authors have no competing interests. **Data and materials availability:** Reagents and materials presented in this study are available from the corresponding authors under a materials transfer agreement with the University of Cape Town.

References.

1. Davies, M.A., *et al.* Outcomes of laboratory-confirmed SARS-CoV-2 infection during resurgence driven by Omicron lineages BA.4 and BA.5 compared with previous waves in the Western Cape Province, South Africa. *Int J Infect Dis* **127**, 63-68 (2022).
2. Johns Hopkins University Center for Systems Science and Engineering. Accessed on: 18 December 2022. Available at: https://coronavirus.jhu.edu/map.html (2022).
3. Cai, J., *et al.* Modeling transmission of SARS-CoV-2 Omicron in China. *Nat Med* **28**, 1468-1475 (2022).
4. Chen, X., *et al.* Estimation of disease burden and clinical severity of COVID-19 caused by Omicron BA.2 in Shanghai, February-June 2022. *Emerg Microbes Infect* **11**, 2800-2807 (2022).
5. Colnago, M., *et al.* Risk factors associated with mortality in hospitalized patients with COVID-19 during the Omicron wave in Brazil. *Bioengineering (Basel)* **9**(2022).
6. Gautret, P., *et al.* The severity of the first 207 infections with the SARS-CoV-2 Omicron BA.2 variant, in Marseille, France, December 2021-February 2022. *J Med Virol* **94**, 3494-3497 (2022).
7. Jassat, W., *et al.* Difference in mortality among individuals admitted to hospital with COVID-19 during the first and second waves in South Africa: a cohort study. *The Lancet. Global health* **9**, e1216-e1225 (2021).
8. Maruotti, A., Ciccozzi, M. & Jona-Lasinio, G. COVID-19-induced excess mortality in Italy during the Omicron wave. *IJID Reg* **4**, 85-87 (2022).
9. Maslo C, M.A., Laubscher A, Toubkin M, Sitharam L, Feldman C, Richards GA. COVID-19: A comparative study of severity of patients hospitalized during the first and the second wave in South Africa. *MedRXiv* (2021).
10. Ward, I.L., *et al.* Risk of covid-19 related deaths for SARS-CoV-2 Omicron (B.1.1.529) compared with Delta (B.1.617.2): retrospective cohort study. *BMJ* **378**, e070695 (2022).
11. Fontana, L.M., Villamagna, A.H., Sikka, M.K. & McGregor, J.C. Understanding viral shedding of severe acute respiratory coronavirus virus 2 (SARS-CoV-2): Review of current literature. *Infect Control Hosp Epidemiol* **42**, 659-668 (2021).
12. Ramos-Rincon, J.M., *et al.* Pathological findings associated with SARS-CoV-2 on postmortem core biopsies: correlation with clinical presentation and disease course. *Front Med* **9**, 874307 (2022).
13. Stein, S.R., *et al.* SARS-CoV-2 infection and persistence in the human body and brain at autopsy. *Nature* **612**, 758-763 (2022).
14. Basile, K., *et al.* Cell-based culture informs infectivity and safe de-isolation assessments in patients with coronavirus disease 2019. *Clin Infect Dis* **73**, e2952-e2959 (2021).
15. Berengua, C., *et al.* Viral culture and immunofluorescence for the detection of SARS-CoV-2 infectivity in RT-PCR positive respiratory samples. *J Clin Virol* **152**, 105167 (2022).
16. Bullard, J., *et al.* Predicting infectious severe acute respiratory syndrome coronavirus 2 from diagnostic samples. *Clin Infect Dis* **71**, 2663-2666 (2020).
17. Lan, L., *et al.* Positive RT-PCR test results in patients recovered from COVID-19. *JAMA* **323**, 1502-1503 (2020).
18. Ling, Y., *et al.* Persistence and clearance of viral RNA in 2019 novel coronavirus disease rehabilitation patients. *Chin Med J* **133**, 1039-1043 (2020).
19. Santos Bravo, M., *et al.* Viral culture confirmed SARS-CoV-2 subgenomic RNA value as a good surrogate marker of infectivity. *J Clin Microbiol* **60**, e0160921 (2022).
20. Singanayagam, A., *et al.* Duration of infectiousness and correlation with RT-PCR cycle threshold values in cases of COVID-19, England, January to May 2020. *Euro surveillance* **25**(2020).
21. van Kampen, J.J.A., *et al.* Duration and key determinants of infectious virus shedding in hospitalized patients with coronavirus disease-2019 (COVID-19). *Nat Commun* **12**, 267 (2021).
22. Wolfel, R., *et al.* Virological assessment of hospitalized patients with COVID-2019. *Nature* **581**, 465-469 (2020).
23. Young, B.E., *et al.* Viral dynamics and immune correlates of coronavirus disease 2019 (COVID-19) severity. *Clin Infect Dis* **73**, e2932-e2942 (2021).

24. Killingley, B., *et al.* Safety, tolerability and viral kinetics during SARS-CoV-2 human challenge in young adults. *Nat Med* **28**, 1031-1041 (2022).
25. Merad, M., Blish, C.A., Sallusto, F. & Iwasaki, A. The immunology and immunopathology of COVID-19. *Science* **375**, 1122-1127 (2022).
26. Bhimraj A, M.R., Shumaker AH, Baden L, Cheng VC, Edwards KM, Gallagher JC, Gandhi RT, Muller WJ, Nakamura MM, O'Horo JC, Shafer RW, Shoham S, Murad MH, Mustafa RA, Sultan S, Falck-Ytte Y. IDSA Guidelines on the Treatment and Management of Patients with COVID-19. Accessed on: 18 December 2022. Available at: https://www.idsociety.org/practice-guideline/covid-19-guideline-treatment-and-management/#Recommendations15-17:Remdesivir. **2022**.
27. Consortium, W.H.O.S.T. Remdesivir and three other drugs for hospitalised patients with COVID-19: final results of the WHO Solidarity randomised trial and updated meta-analyses. *Lancet* **399**, 1941-1953 (2022).
28. Beigel, J.H., *et al.* Remdesivir for the Treatment of Covid-19 - Final Report. *The New England journal of medicine* **383**, 1813-1826 (2020).
29. Lapadula, G., *et al.* Remdesivir Use in Patients Requiring Mechanical Ventilation due to COVID-19. *Open Forum Infect Dis* **7**, ofaa481 (2020).
30. Pasquini, Z., *et al.* Effectiveness of remdesivir in patients with COVID-19 under mechanical ventilation in an Italian ICU. *J Antimicrob Chemother* **75**, 3359-3365 (2020).
31. Ragab, D., Salah Eldin, H., Taeimah, M., Khattab, R. & Salem, R. The COVID-19 cytokine storm; what we know so far. *Front Immunol* **11**, 1446 (2020).
32. Tay, M.Z., Poh, C.M., Renia, L., MacAry, P.A. & Ng, L.F.P. The trinity of COVID-19: immunity, inflammation and intervention. *Nat Rev Immunol* **20**, 363-374 (2020).
33. van de Veerdonk, F.L., *et al.* A guide to immunotherapy for COVID-19. *Nat Med* **28**, 39-50 (2022).
34. Wang, E.Y., *et al.* Diverse functional autoantibodies in patients with COVID-19. *Nature* **595**, 283-288 (2021).
35. Deinhardt-Emmer, S., *et al.* Early postmortem mapping of SARS-CoV-2 RNA in patients with COVID-19 and the correlation with tissue damage. *Elife* **10** (2021).
36. Andrews, S. FastQC: A Quality Control Tool for High Throughput Sequence Data. Accessed on 7th December 2022. Available at: https://www.bioinformatics.babraham.ac.uk/projects/fastqc/ (2010).
37. Dobin, A., *et al.* STAR: ultrafast universal RNA-seq aligner. *Bioinformatics* **29**, 15-21 (2013).
38. Howe, K.L., *et al.* Ensembl 2021. *Nucleic Acids Res* **49**, D884-D891 (2021).
39. Robinson, M.D., McCarthy, D.J. & Smyth, G.K. edgeR: a Bioconductor package for differential expression analysis of digital gene expression data. *Bioinformatics* **26**, 139-140 (2010).
40. Huber, W., *et al.* Orchestrating high-throughput genomic analysis with Bioconductor. *Nat Methods* **12**, 115-121 (2015).
41. Wu, T., *et al.* clusterProfiler 4.0: A universal enrichment tool for interpreting omics data. *Innovation (Camb)* **2**, 100141 (2021).